ENGINEERING TRANSACTIONS • *Engng. Trans.* • **65**, 1, 45–51, 2017
Polish Academy of Sciences • Institute of Fundamental Technological Research (IPPT PAN)
National Engineering School of Metz (ENIM) • Poznan University of Technology

Stability of an Innovative Cold-Formed GEB Section

Agnieszka ŁUKOWICZ, Marcin KRAJEWSKI

Gdańsk University of Technology
Faculty of Civil and Environmental Engineering
Narutowicza 11/12, 80-233 Gdańsk, Poland
e-mail: markraje@pg.gda.pl

This paper is focused on the numerical analysis and experimental test of stability of the cold-formed profile with an innovative GEB cross-section. For the shell model of the axially compressed member, the linear buckling analysis and the nonlinear static analysis were carried out. In the numerical research, the buckling load and the limit load for variable section heights were obtained. Some of the results were compared with the GEB member bearing capacity calculated on the basis of PN-EN 1993-1-1 Eurocode 3 requirements.

Key words: cold-formed profiles, buckling load, limit load.

1. Introduction

Cold-formed steel sections are generally used as secondary elements like purlins or sheeting. In this paper, an innovative GEB cross-section was developed and it may serve as a primary load-bearing member in fabricated steel panels and trusses. The stability of typical cold-formed open steel sections (e.g., bended C- and Z-sections) have been studied in recent years [1], however according to the European Standards requirements every new section shape should be tested [2]. The application of the GEB member in metal building structures depends on configuration of the optimal dimensional parameters. These parameters are in this case associated with the cross-section production possibilities. The paper is devoted to the numerical and experimental investigation of the stability of a steel GEB section (Fig. 1a). The present analysis is a continuation of previous researches [3, 4]. For the axially compressed GEB member, the linear buckling analysis and nonlinear static analysis (geometric and material nonlinearity) were carried out. Also the experimental test was conducted to verify the results obtained from the numerical shell models.

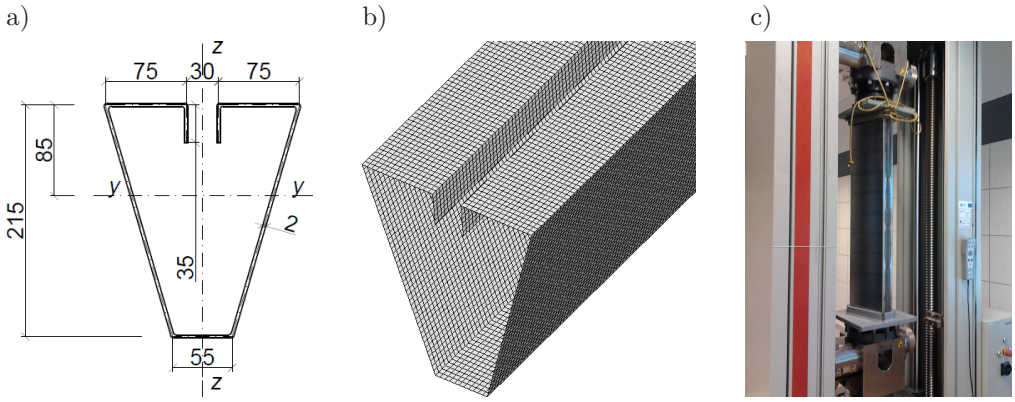

FIG. 1. GEB section: a) geometric details, b) shell model detail, c) experimental set-up.

2. Description of the GEB profile

The length of the tested GEB member was equal to $L = 6.0$ m (numerical analysis) and $L = 1.0$ m (numerical and experimental research). In the numerical research, it was assumed that bottom wall width (55 mm) and distance between vertical parallel walls (30 mm) were constant (Fig. 1). The cross- section height varied. The experimental test was conducted by the Zwick-Roell Z400 strength-testing machine. Due to the complicated cross-section shape, the experimentally tested sample has been manufactured with two steel sheets assembled together by longitudinal butt weld.

3. Numerical model

In the numerical analysis, the FEM was used to solve the problem. About 29 000, four-node shell elements *QUAD4* [5] were used. The minimum element size was 5.0×5.0 mm^2. The arc-length method was used to apply loading. It was assumed that the structure was pinned at marginal supports. The structure was made of DC04 grade steel and the material characteristics were determined using a separate testing ($E = 178$ GPa, $f_y = 206$ MPa). The assumed Poisson's ratio was equal to 0.3 [2]. In the numerical analysis (GMNIA), the bi-linear (elasto-plastic) body model was implemented, i.e., for the uniaxial model: $\sigma = E\varepsilon$ – first phase ($\sigma < f_y$) and $\sigma = f_y$ – second phase (σ-stress, ε-strain).

4. Numerical analysis results

The linear buckling analysis results (LBA – structure without imperfection) are presented in Fig. 2 and Table 1. Depending on the GEB section height and

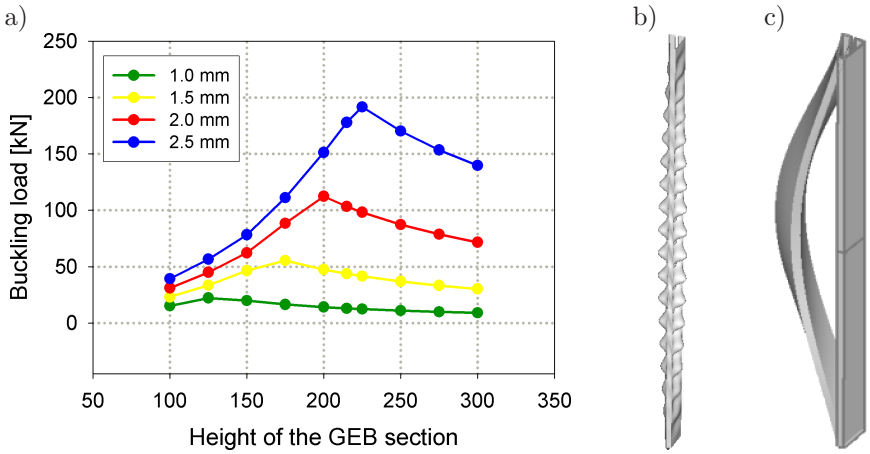

FIG. 2. The linear buckling analysis results: a) relation between buckling load and GEB section height, b) buckling mode for the GEB height $h = 0.215$ m (thickness 2.0 mm) – local deformation, c) buckling mode for the GEB height $h = 0.175$ m (thickness 2.0 mm) – global deformation.

Table 1. Magnitudes of the first buckling loads P_{cr} [kN], gray label – local deformation, white label – global deformation.

GEB section height	GEB thickness			
	1.0 mm	1.5 mm	2.0 mm	2.5 mm
100	15.2	23.1	31.0	39.3
125	22.1	33.4	44.9	56.5
150	19.8	46.4	62.2	78.2
175	16.4	55.3	88.4	111.1
200	14.1	47.5	112.3	151.3
215	12.9	43.6	103.3	177.8
225	12.3	41.5	98.2	191.6
250	10.9	36.9	87.3	170.2
275	9.8	33.2	78.7	153.5
300	9	30.2	71.6	139.7

thickness, the form of the first buckling mode (corresponding to the first buckling load) can be described as local deformation of the structure (several waves at each wall along the GEB member) or global deformation of the member (flexural torsional buckling). It is worth noting that the buckling load for the structure increased due to the increase of GEB section height, but only to the threshold GEB section height (depended on the wall thickness). For the profiles with higher walls in the LBA results, the local buckling appeared and the buckling load decreased.

The nonlinear static analyses (GMNIA – geometric and material nonlinearity) were carried out for the shell model of the structure. In each case, as the initial geometric imperfection the deformation in the form of first buckling mode (obtained from LBA) was taken into consideration. The maximum magnitude of the imperfection (maximum total translation) was equal to $L/500$ due to the code requirements [5]. The results are presented in Fig. 3 and Fig. 4. The limit load obtained from the GMNIA increased due to the increase of GEB section height and thickness. For the members with implemented local imperfection (Fig. 2b), the deformation at the limit state had the combined form of several waves along the GEB member and arch curvature in the plane perpendicular to the $y-y$ axis. In this case, for the opened GEB cross-section at the beginning

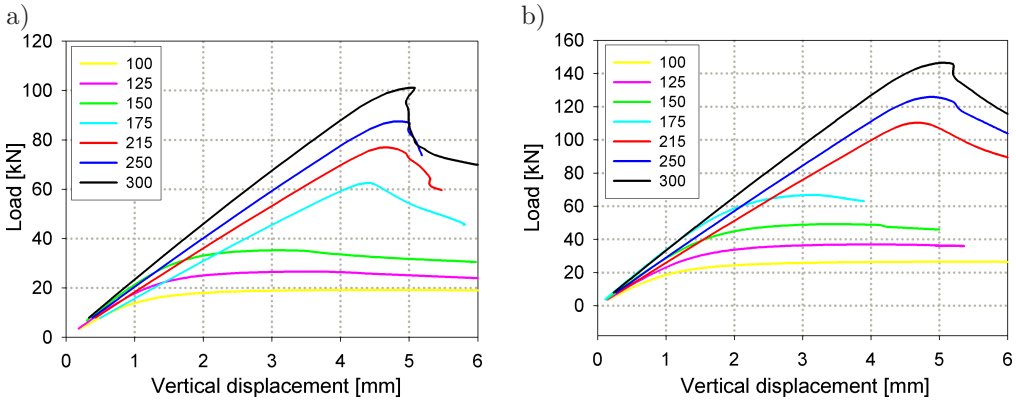

FIG. 3. The loading due to the vertical displacement (of the loaded joint) with respect to the GEB height for: a) section thickness equal to 1.5 mm, b) section thickness equal to 2.0 mm.

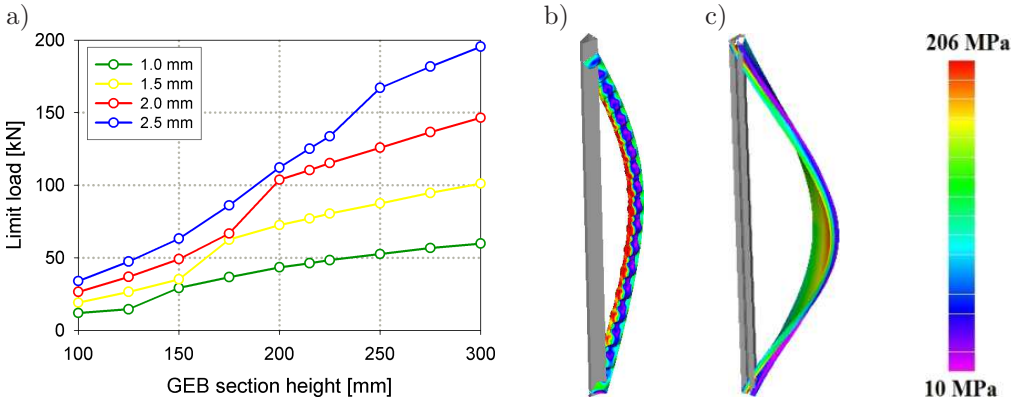

FIG. 4. The nonlinear analysis results: a) limit load vs. GEB height with respect to section thickness, b) deformation at the limit state and HMH stress on outer surface for GEB h = 215 mm, thickness 2.0 mm, c) deformation at the limit state and HMH stress on outer surface for GEB h = 175 mm, thickness 2.0 mm.

of equilibrium path the highest magnitudes of stresses (HMH stress on outer surface of GEB) appeared at the bottom cross-section wall (55 mm – constant width). The plastic range at the limit state is presented in Figs. 4b or 4c (for initial geometric imperfection see Fig. 2c).

5. Experimental analysis results

The length of the tested GEB member was equal to $L = 1.0$ m (cross-section – Fig. 1a). The results of the experimental and numerical research are presented in Figs. 5 and 6. In the numerical analysis (GMNIA) carried out for

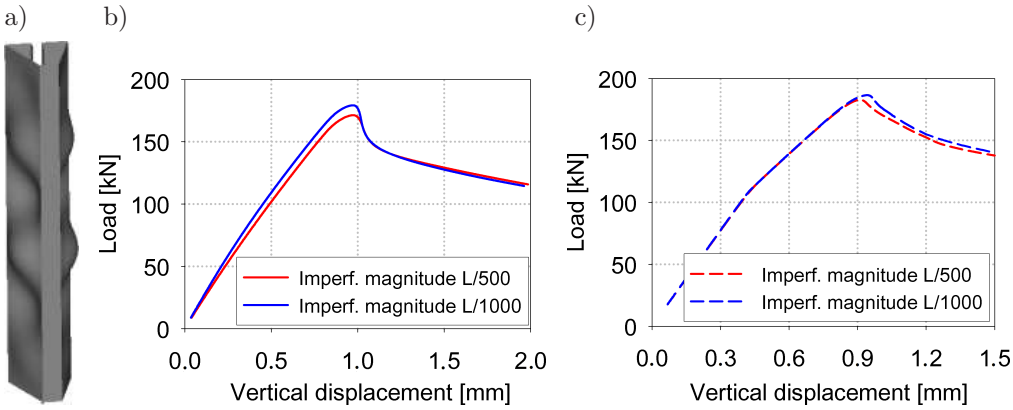

Fig. 5. The numerical analysis results performed for the experimentally tested GEB member: a) LBA – first buckling mode, $P_{cr} = 107$ kN, b) GMNIA – imperfection I, c) GMNIA – imperfection II.

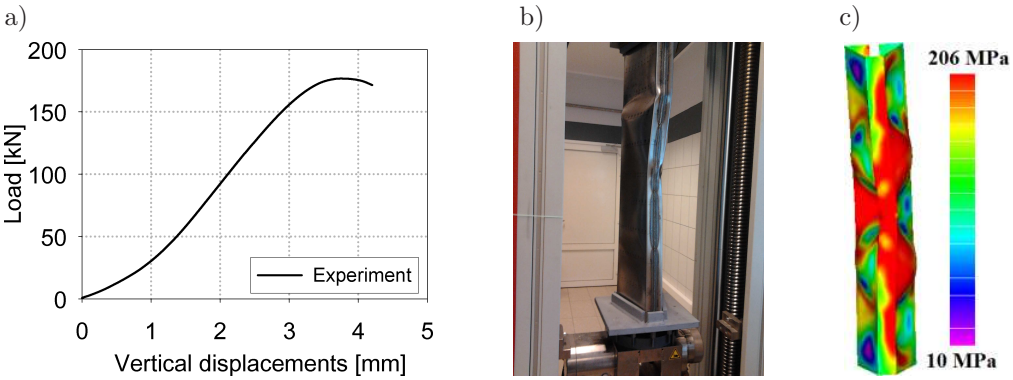

Fig. 6. The experimental test and numerical analysis results: a) loading vs. vertical displacement at the top joint obtained from the experimental research, b) GEB deformation at the limit state – experimental test, c) deformation and stress state for the limit load – GMNIA imperfection II – HMH stress on outer surface of GEB.

the experimentally tested sample, two kinds of initial geometric imperfections were considered. The first imperfection (imperfection I) was implemented to the structure on the basis of the LBA results (first buckling mode $P_{\mathrm{cr}} = 107$ kN – Fig. 5a), and the second imperfection (imperfection II) was the global arch curvature (in the plane perpendicular to the $z{-}z$ axis), which was observed after member assembling on the experimental set-up. The assumed maximum magnitude of the imperfections was equal to $L/500$ and $L/1000$. In this case, the differences between the limit load obtained from GMNIA were up to 9%.

6. GEB bearing capacity due to code EC3 requirements

On the basis of code [2, 6, 7] requirements, the calculations for the axially compressed member ($L = 6.0$ m, $h = 215$ mm – Fig. 1a) were performed. The authoritative effective area (A_{eff}) and buckling load (P_{cr}* – corresponding to the global – flexural-torsional buckling) were taken into account. The results are presented in Table 2.

Table 2. GEB member characteristics due to code EC3, GEB $h = 215$ mm, χ – buckling factor.

GEB section thickness [mm]	A [cm^2]	A_{eff} [cm^2]	P_{cr}* [kN]	χ	$\mathrm{N_{bRd}}$ [kN]
1.0	7.23	2.5	65.2	0.67	34.4
1.5	10.84	5.33	103.8	0.58	63.6
2.0	14.46	8.61	141	0.52	92.7
2.5	18.07	11.95	177.8	0.49	120.9

7. Conclusions

On the basis of the LBA results, one can conclude that there was a threshold GEB section height that ensures maximum magnitude of buckling load. In every case, the limit load obtained from the GMNIA increased with an increase of cross-section height. The profile bearing capacity calculated due to codes requirements was lower (25% for a thickness of 1 mm or 4% for a thickness of 2.5 mm) with comparison to the GMNIA results.

The differences between loading magnitudes obtained from the numerical results and experimental tests were up to 5%, depending on the shape and magnitude of imperfection. The stiffness of the supporting elements located at the experimental set-up (boundary conditions) was not taken into account in the nonlinear analysis. This might be the reason for large discrepancies between

the displacement magnitudes obtained from the numerical and experimental test results.

References

1. Schafer B.W., *Local, distortional, and Euler buckling of thin-walled columns*, Journal of Structural Engineering, **128**(3): 289–299, 2002, doi: 10.1061/(ASCE)0733-9445(2002)128:3(289).
2. PN-EN 1993-1-3 Eurocode 3 (2006): Design of steel structures. Part 1–3: General rules – Supplementary rules for cold-formed members and sheeting.
3. Łukowicz A., Urbańska-Galewska E., Deniziak P., Gordziej-Zagórowska M., *Classification of restraints in the optimization problem of a cold-formed profile*, Advances in Science and Technology, **9**(28): 61–67, 2015, doi: 10.12913/22998624/60785.
4. Łukowicz A., Urbańska-Galewska E., Gordziej-Zagórowska M., *Experimental testing of innovative cold-formed GEB section*, Civil and Environmental Engineering Reports, **16**(1): 129–140, 2015, doi: 10.1515/ceer-2015-0010.
5. Femap with Nastran N.X., *Finite element modeling and post-processing,* Version 10.1.1., Siemens Product Lifecycle Management Software Inc., 2009.
6. PN-EN 1993-1-1 Eurocode 3, Design of steel structures. Part 1–1: General rules and rules for buildings, 2006.
7. PN-EN 1993-1-5 Eurocode 3, Design of steel structures. Part 1–5: General rules – Plated structural elements, 2006.

Received October 15, 2016; accepted version November 16, 2016.